Ferreira, Leonardo Nogueira; Mumtaz, Haroon; Pinter, Gabor

Working Paper

A millennium of UK business cycles: Insights from structural VAR analysis

Working Paper, No. 995

Provided in Cooperation with:
School of Economics and Finance, Queen Mary University of London

Suggested Citation: Ferreira, Leonardo Nogueira; Mumtaz, Haroon; Pinter, Gabor (2025) : A millennium of UK business cycles: Insights from structural VAR analysis, Working Paper, No. 995, Queen Mary University of London, School of Economics and Finance, London

This Version is available at:
https://hdl.handle.net/10419/339519

A Millennium of UK Business Cycles: Insights from Structural VAR Analysis

Leonardo N. Ferreira, Haroon Mumtaz, Gabor Pinter

Working Paper No. 995 November 2025 ISSN1473-0278

School of Economics and Finance

Queen Mary University of London

A Millennium of UK Business Cycles: Insights from Structural VAR Analysis*

Leonardo N. Ferreira † Haroon Mumtaz ‡ Gabor Pinter §

November 19, 2025

Abstract

We study macroeconomic fluctuations in the United Kingdom over seven centuries (1271–2022) using a time-varying VAR with stochastic volatility. We identify business cycle shocks as innovations explaining the largest share of future output variance. Before 1900, these shocks display a stagflationary, supply-driven pattern, while post-1900 shocks become demand-driven, raising both output and inflation. Output volatility declines over time, peaking in the seventeenth century. Monetisation had large real effects in the sixteenth and seventeenth centuries, shifting to more inflationary impacts thereafter. Our results highlight how business cycle dynamics evolve with institutional, monetary, and structural transformations.

Keywords: Long-run data; Business Cycle shock; time-varying VAR.

JEL Codes: C32; E32; E43.

*We thank participants of the Workshop in Empirical and Theoretical Economics at King's College London for their useful comments. The views expressed in this paper are those of the authors and do not represent those of the Bank for International Settlements, the Central Bank of Brazil, or any of their Committees.

†Central Bank of Brazil. Email: leonardo.ferreira@bcb.gov.br

‡Queen Mary University of London. Email: h.mumtaz@qmul.ac.uk

§Bank for International Settlements. Email: gabor.pinter@bis.org

1 Introduction

Macroeconomic fluctuations have been a persistent feature of human economic history. Yet, modern empirical business cycle research typically restricts attention to the post-World War II era, often due to data availability and methodological convenience. As a result, our understanding of macroeconomic dynamics is largely derived from a relatively short and historically exceptional period.

In this paper, we take a long-run perspective and study the evolution of macroeconomic fluctuations in the United Kingdom over more than seven centuries, from 1271 to 2022. By combining historical macroeconomic data on output, inflation, and money with a structural time-varying vector autoregression (TVP-VAR) framework that accounts for measurement error in long-run macroeconomic series, we provide novel evidence on the changing nature of business cycles.

The long time span allows us to investigate a fundamental question: have the sources and propagation mechanisms of business cycles changed over time? Drawing inspiration from recent work by Angeletos et al. (2020), we identify the main business cycle shock in each year as the innovation that explains the largest share of short-term GDP growth variance. This agnostic approach avoids imposing modern structural interpretations on earlier eras. We estimate a time-varying VAR with stochastic volatility and fat-tailed shocks, enabling us to capture drifting macroeconomic regimes, levels of uncertainty, and non-Gaussian features that characterize pre-modern economies. Our analysis yields five main results.

First, our findings reveal a striking historical transformation in the nature of business cycle shocks. Prior to 1900, macroeconomic fluctuations were dominated by supply-side disturbances, with negative shocks reducing output per capita and raising prices – a stagflationary pattern consistent with historical famines, wars, and climate events. In contrast, from the early twentieth century onward, business cycle shocks take on a demand-driven character, producing positive co-movement between output and inflation. This regime shift coincides with the rise of fiat money, modern central banking, and active fiscal-monetary stabilization policies (Reinhart and Rogoff, 2008, 2013).

Second, our results reveal a long-run decline in output volatility, with the 17th century marking the peak of economic instability over the past millennium due to wars, political upheaval, and climatic shocks (Parker, 2013). Volatility was lower both before and after this period. Even the turbulent business cycles of the twentieth century show smaller output fluctuations than the 17th century, except for the temporary spike during COVID-19. Overall, this pattern suggests a centuries-long Great "Moderation" (Kim and Nelson, 1999; McConnell and Perez-Quiros, 2000; Primiceri, 2005), as economic development and stabilising institutions gradually reduced the amplitude of business cycle fluctuations.

Third, during the sixteenth and seventeenth centuries, money supply variation had substantial real effects, consistent with historical accounts that monetisation facilitated market transactions and economic expansion (Palma, 2018a,b, 2022). However, while money variation explained a significant share of business cycle fluctuations in earlier centuries, its influence became increasingly inflationary from the eighteenth century onward, consistent with a transition towards demand-dominated cycles.

Fourth, our sign-restricted VAR results for the post-1700 period show that aggregate demand disturbances capture the effects of both pure demand shocks and money supply shocks. While pure demand shocks account for a slightly larger share of output and price variation, money supply shocks also play a significant role, particularly in explaining fluctuations in money itself.

Fifth, we find that the shift toward inflationary business cycle shocks is more closely linked to the expansion of base money than to financial deepening per se. While the M4/M0 ratio – our proxy for financial development – rises sharply after 1970, the demand-type characteristics of business cycle shocks had already emerged during the late nineteenth century.

By tracing the evolution of British business cycles from the medieval period to the present, our paper highlights the importance of long-run historical data for macroeconomic analysis. We demonstrate that business cycle dynamics are not stable or universal, but instead reflect the institutional, monetary, and structural environment in which they unfold. These insights are particularly relevant for interpreting recent macroeconomic shocks – such as COVID-19 and inflation surges – within a broader historical context.

Related Literature This paper primarily contributes to the literature that seeks the drivers of business cycles. Empirical studies of modern business cycles argue that business cycles are primarily driven by demand shocks, thereby challenging the more traditional view from Real Business Cycle (RBC) models (Kydland and Prescott 1982). The finding emerges both from VAR-type models (Shapiro and Watson 1988; Blanchard and Quah 1989; Gali 1999) as well as from more structural models (Smets and Wouters 2007; Christiano et al. 2014). More recently, the findings of Angeletos et al. (2020) support the existence of a main business-cycle driver which fits the notion of an aggregate demand shock. Our work extends this analysis to multiple centuries, showing how the main business-cycle shock has changed from supply-like to demand-like around 1850-1900.

Our analysis of a nearly millennium long dataset for the UK is inspired by several recent papers (Hansen et al., 2020; Schmelzing, 2020; Nason and Smith, 2023; Rogoff et al., 2024; Bouscasse et al., 2025). What distinguishes our work is that we model the joint behaviour of price and quantity variables, allowing us to distinguish between supply- and demand-type shocks in the spirit of modern structural macroeconomic models.[1]

2 Data

Our dataset is annual, spanning the period from 1271 to 2022.[2] Our source is "A millennium of macroeconomic data", compiled by Thomas and Dimsdale (2018). This database contains a broad set of macroeconomic and financial data for the UK, in some cases, from 1086 to 2016. We select the three variables that best characterise the macroeconomic dynamics throughout the centuries and update them up to 2022. These are GDP per capita, CPI, and money (M0) per capita.

[1] For example, Nason and Smith (2023) analysis inflation dynamics in a univariate framework, Rogoff et al. (2024) focuses on the long-run dynamics of interest rates, and Bouscasse et al. (2025) focuses on real variables and does not study inflation dynamics.

[2] As described in the appendix, we use the first 50 observations as training sample.

3 Empirical Model

We use a time-varying VAR with stochastic volatility and fat tails to model the dynamics of these variables:

$$Y_t = c_t + \sum_{j=1}^{P} b_{j,t} Y_{t-j} + \Sigma_t^{1/2} e_t, \quad e \sim N(0,1), \tag{1}$$

where $Y_t = \{\Delta y_t, \Delta p_t, \Delta m_t\}$ and $L = 2$ represents the lag length. Following Cogley and Sargent (2005) and Primiceri (2005), the coefficients are time-varying with $\Phi_t = \Phi_{t-1} + Q^{1/2}\eta_t$, where $\Phi_t = vec([c_t, b_{j,t}])$ represents the time-varying coefficients stacked in one vector and η_t is a conformable vector of innovations. As in Primiceri (2005), the covariance matrix of the innovations v_t is factored, $\Sigma_t = A_t^{-1} H_t A_t^{-1'}$, where the non-zero and non-one elements of A_t follow a random walk, $\alpha_{ij,t} = \alpha_{ij,t-1} + Q_\alpha^{1/2} v_t$. As we also model fat tails, H_t is a diagonal matrix with elements $\sigma_{i,t}^2 \frac{1}{\lambda_{i,t}}$ for $i = 1, 2, 3$. Here, $\ln \sigma_{i,t}^2 = \ln \sigma_{i,t-1}^2 + g_i^{1/2} z_t$ and $\lambda_{i,t}$ are weights that lead to a scale mixture of normals such that the orthogonalised residuals $A_t u_t \sim T(0, \sigma_{i,t}, v_{\lambda,i})$. As shown by Geweke (1993) this scale mixture can be obtained if one assumes that $p(\lambda_k) = \prod_{i=1}^{T} \Gamma(1, v_{\lambda,k})$.

Modelling fat tails is particularly important in our context, as it provides robustness against extreme observations that may arise from measurement error or archival uncertainty in pre-modern macroeconomic data (Muller et al., 2025). Rather than treating these outliers as structural shifts, the t-distribution allows the model to downweight their influence without distorting the underlying signal.[3]

3.1 Identification

Building on Uhlig (2004); Barsky and Sims (2011); Kurmann and Otrok (2013); Kurmann and Sims (2021); Chahrour et al. (2023), we identify the business cycle shock as the VAR innovation that makes the largest contribution to the forecast error variance (FEV) of Δy_t at horizon 1. Angeletos et al. (2020) show this is equivalent to identifying, in the frequency domain, the shock that dominates the business-cycle frequencies (1.5-8 years).

[3]This feature is also valuable for handling modern data outliers, such as those arising during the Covid-19 pandemic.

We decompose Σ such that $\Omega\Omega' = \Sigma$ where Ω represents a contemporaneous impact matrix. Ω can be written as $\Omega = \tilde{\Omega}Q$ where Q is an orthonormal matrix that rotates $\tilde{\Omega}$, the Cholesky decomposition of Σ. The structural moving average representation of the VAR model is then given by:

$$Y_t = B(L)\Omega\varepsilon_t, \tag{2}$$

where ε_t denotes the orthogonal shocks.

The k-period-ahead forecast error of the ith variable is defined as

$$Y_{it+k} - \hat{Y}_{it+k} = e_1 \left[\sum_{j=0}^{k-1} B_j \tilde{\Omega} Q \varepsilon_{t+k-j} \right], \tag{3}$$

where e_1 is a selection vector that picks out in the set of variables. The proposed identification scheme thus amounts to finding the column of Q that solves the following maximization problem:

$$\arg\max_{Q_1} e_1' \left[\sum_{k=0}^{K} \sum_{j=0}^{k-1} B_j \tilde{\Omega} Q_1 Q_1' \tilde{\Omega}' B_j' \right] e_1, \tag{4}$$

such that $Q_1'Q_1 = 1$, where Q_1 is the column of Q that corresponds to the shock that explains the largest proportion of the FEV of the first variable in the VAR: Δy_t.

4 Results

The dynamic effects of business cycle shocks over time are vividly illustrated in Figure 1, which presents the impulse response functions (IRFs) and forecast error variance decompositions (FEVDs) associated with these shocks. Figure 1a shows the IRFs cumulated over the 5-year horizon corresponding to a business cycle shock that is normalised to have a unit standard deviation. The top panel of Figure 1 illustrates the responses of GDP per capita, the middle panel shows the responses of CPI, and the bottom panel depicts the responses of money stock per capita. Moreover, the black lines in Figure 2 represent the estimated time-varying stochastic volatility, while the blue lines capture the estimated volatility conditional on the identified business cycle shock.

Supply Shocks as Drivers of Pre-Modern Business Cycles In earlier centuries, business cycle shocks exhibit a classic supply-side pattern, where output declines while inflation rises (Figure 1a). This pattern aligns with the frequent occurrence of wars and famines during this period.[4] While extreme events such as the Black Death (1348–50) resulted in a larger contraction in population than in output—thereby increasing output per capita—our estimates indicate that typical supply-side shocks during this era tended to reduce output per capita while driving up prices. Prior to 1500, agricultural production, particularly arable farming, was highly volatile due to weather-related shocks, while industrial production and commercial or monetary factors contributed minimally to growth dynamics (Broadberry et al., 2012).

The Most Volatile Economic Period The 17th century stands out as the period with the strongest propagation of business cycle shocks exhibiting supply-side characteristics. During this time, a realization of the shock had the largest effects on GDP and CPI, with changes of approximately 5% and -4%, respectively. This aligns with the significant economic, social, and political upheaval of the era, as reflected in the estimated stochastic volatility of output, which peaks during this period (top panel of Figure 2). The 17th century was marked by a global crisis characterized by frequent wars, climate change, and widespread catastrophes (Parker, 2013).[5] Even in comparison to the 20th century, the business cycle volatility of this period remains unparalleled.

The behaviour of inflation and money offers valuable insights into the historical relationship between monetary drivers of inflation—or the lack thereof—in earlier centuries. The negative conditional comovement between inflation and money growth suggests that money supply shocks, as posited by the quantity theory of money Friedman (1956), are

[4] Appendix Figure E.1 highlights significant realisations of the business cycle shocks associated with well-documented historical events characterized by supply-side dynamics.

[5] Parker (2013) argues that the "Little Ice Age" brought prolonged cooling, erratic weather patterns, and repeated harvest failures, leading to famines and economic instability. These environmental stresses coincided with the English Civil War (1642–1651) and widespread rebellions across Europe, which disrupted trade, devastated agricultural output, and strained public finances. The interplay between climate-induced scarcity and human-driven conflict created a "fatal synergy" that destabilized the economy, reduced population levels, and fuelled social unrest. In the UK, these dynamics were further exacerbated by political upheaval, including the execution of Charles I and the subsequent establishment of the Commonwealth. This combination of natural disasters and human agency intensified the magnitude and frequency of economic shocks, making the 17th century one of the most volatile periods in British history.

Figure 1: The effects of business cycle shocks over centuries

(a) Impulse response functions

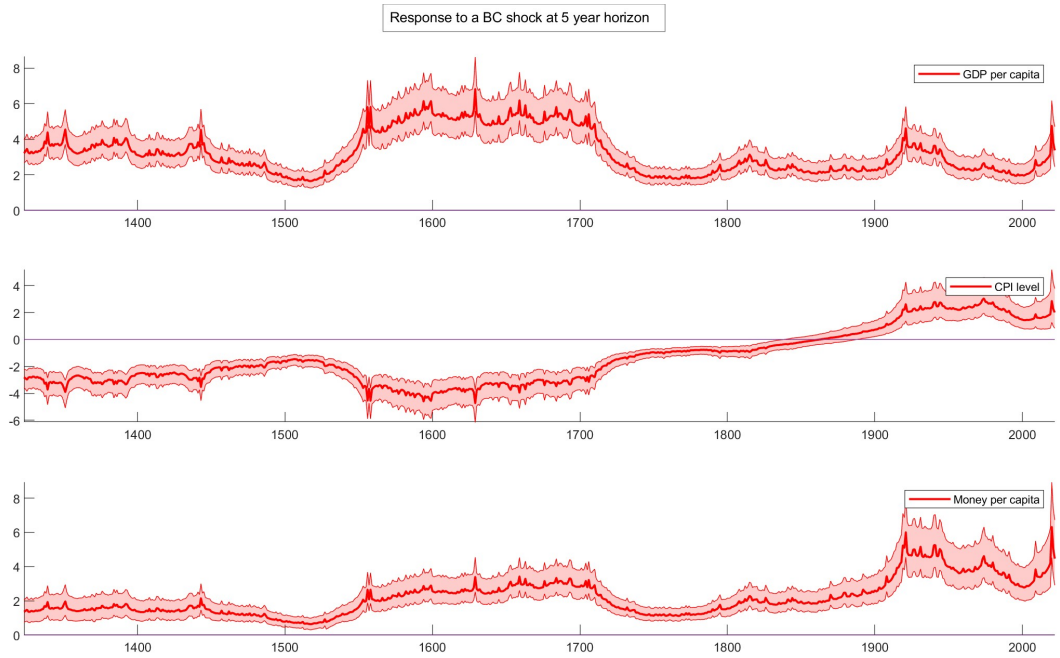

(b) Forecast error variance decomposition

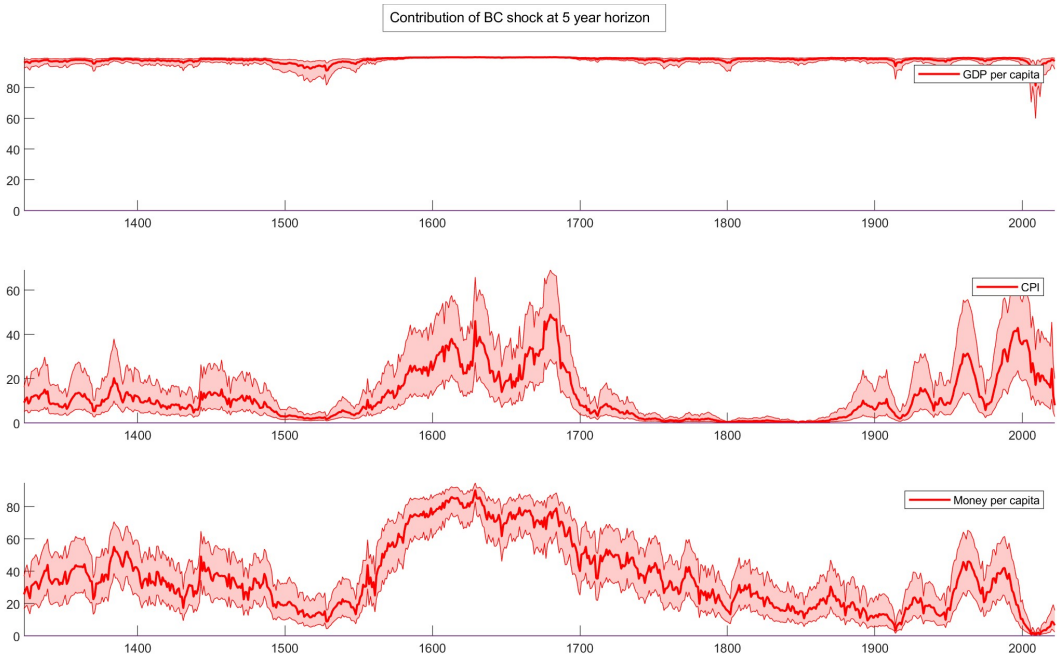

Notes: The pink shaded areas represent the 68 percent credible sets and the red lines depict the medians.

Figure 2: Conditional Volatility

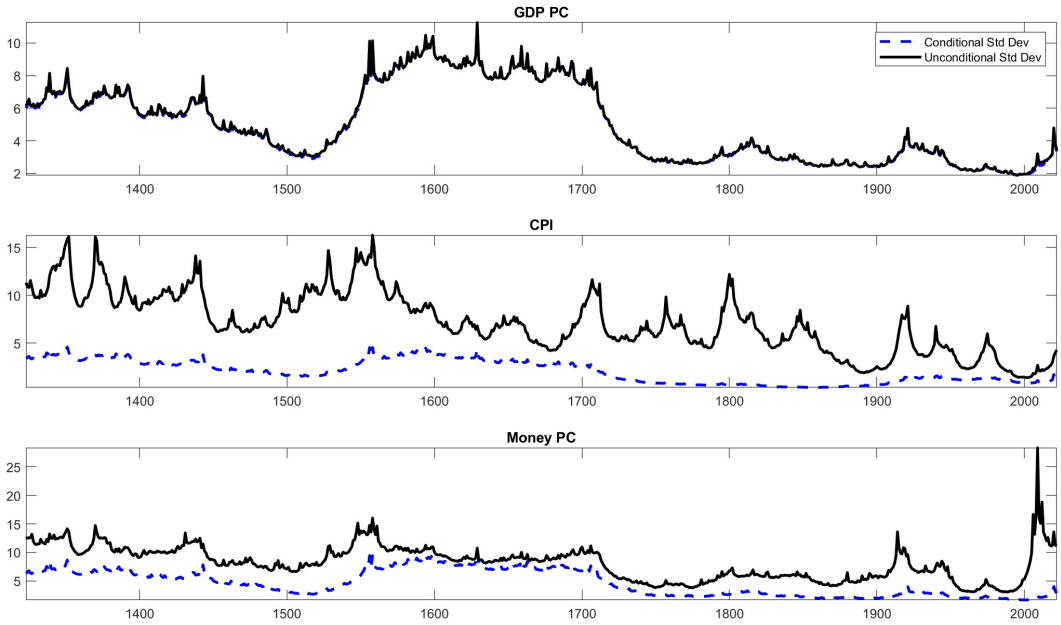

Notes: The dashed blue lines are the estimates of the time-varying volatilities of each variable conditional on the business cycle shock. The solid black lines are the estimates of the unconditional volatilities of each of these variables.

unlikely to be the primary drivers of the identified business cycle shocks. To contextualise this finding, historians have long debated whether the inflow of precious metals from the Americas fuelled the elevated inflation levels of the 16th century (Hamilton (1934)) or whether inflationary pressures were instead driven by real factors, such as demographic and resource constraints (Ramsey (1971)).[6]

Our empirical results do not definitively corroborate or refute either hypothesis, as the forecast error variance in inflation (middle panel of Figure 1b) attributed to business cycle shocks remains limited during most of the 16th century, when the price surge occurred.[7]Specifically, business cycle shocks explain, at most, around 20% of the forecast error variance in inflation during the 16th century and approximately 40% during the 17th century. However, the variance in inflation that can be attributed to business cycle shocks appears inconsistent with channels related to the quantity theory of money, given the negative comovement between inflation and money growth induced by these shocks during this period.

[6]See McCloskey (1972) for a review of the debate.
[7]See Figure 5.01 of Broadberry et al. (2015).

The Real Effects of Monetisation in the 16th and 17th Centuries Despite the limited ability of the business cycle shock to explain inflation variation, it accounts for a substantial portion of the variation in money during the 17th century. Beginning in the mid-16th century, the forecast error variance in money rises from around 20% to nearly 80% by 1600 and remains elevated throughout the 17th century. This significant increase in the conditional comovement between the business cycle and money aligns with the earlier inflow of precious metals into the macroeconomy, lending empirical support to the argument that "monetisation greased the wheels of economic activity" (Abad and Palma, 2021). Empirical evidence also highlights the role of increased money supply in stimulating economic growth (Palma, 2018b).[8] A proposed mechanism is that the greater availability of money enhanced market participation and facilitated tax collection (Palma, 2018a).[9] Increased market participation, in turn, encouraged individuals to work additional days and hours, thereby expanding the labor supply—a phenomenon described as "an industrious revolution" (de Vries, 2008). Our findings provide empirical support for these arguments, particularly in demonstrating the unprecedentedly large real effects associated with money variation during the 17th century.

During the period 1700-1900, macroeconomic volatility fell (Figure 2) and the business cycle shocks have a falling explanatory power for money, suggesting that the real effects of monetisation were fading, and the shock has an increasingly inflationary effect during this period (middle panel of Figure 1a). The latter finding suggests an increasingly demand-like characteristic of the business cycle shock, which coincides with the development of the consumer society in Great Britain which was accelerated by the Industrial Revolution (1760–1840). By the Victorian era (1837–1901), consumer culture was firmly established, with growing emphasis on shopping as a social activity and the acquisition of goods as a marker of identity and status (Perkin, 1969).

[8] Endogenous growth models (Romer, 1990; Aghion and Howitt, 1992) extended with monetary features (Aghion et al., 2012; Chu and Cozzi, 2014; Anzoategui et al., 2016; Gil and Iglesias, 2020) provide a theoretical rationale.

[9] Search-based theories of money (e.g. Shi, 1997) could possibly rationalise why increased money growth can increase agents' probability of having a successful match.

Demand Shocks as Drivers of Modern Business Cycles After 1900, the explanatory power of the business cycle shock for inflation rises markedly, consistent with an environment in which inflation becomes more responsive to aggregate demand conditions. Notably, this shift aligns with the broader transition to modern monetary and fiscal frameworks as economies moved away from commodity-based monetary systems, such as the gold standard, toward fiat currency regimes. This transition granted governments greater flexibility to manage aggregate demand through monetary and fiscal policies, leading to inflation dynamics that were increasingly tied to economic cycles. The adoption of these modern frameworks, particularly after World War II, facilitated more active policy interventions, making inflation more sensitive to aggregate demand shocks. This evolution is consistent with historical evidence highlighting the prevalence of inflation crises in the 20th century, driven by fiscal and monetary expansions aimed at stabilizing growth and employment (Reinhart and Rogoff, 2008). Notable recent papers, such as (Smets and Wouters 2007; Christiano et al. 2014), highlight the importance of demand-type shocks in driving business cycle fluctuations. Our results show that the importance of demand shocks as drivers of business cycles is only limited to the twentieth century onwards.

Money Growth and Financial Development in the 20th Century The 20th century witnessed a profound transformation in the relationship between money and macroeconomic dynamics. Figures 3a and 3b illustrate this changing relationship, highlighting the rapid expansion of both narrow money (M0) and broad money (M4) starting in the early twentieth century. This expansion coincides with the emergence of inflationary business cycle shocks, as shown by the blue solid line in Figures 3a. This pattern points to a structural break in the monetary regime and suggests that monetary expansion—whether driven by loose monetary policy or endogenous money demand—has increasingly shaped the inflation-output nexus since 1900 (Reinhart and Rogoff, 2013).

To differentiate between monetary looseness and broader financial deepening, we use the M4/M0 ratio as a proxy for financial development. As illustrated in Figure 3b, this ratio shows a steady increase after 1850, with a sharp acceleration post-1970. Interestingly, during this

Figure 3: Inflationary effects and monetary developments

(a) Inflationary effects and money growth

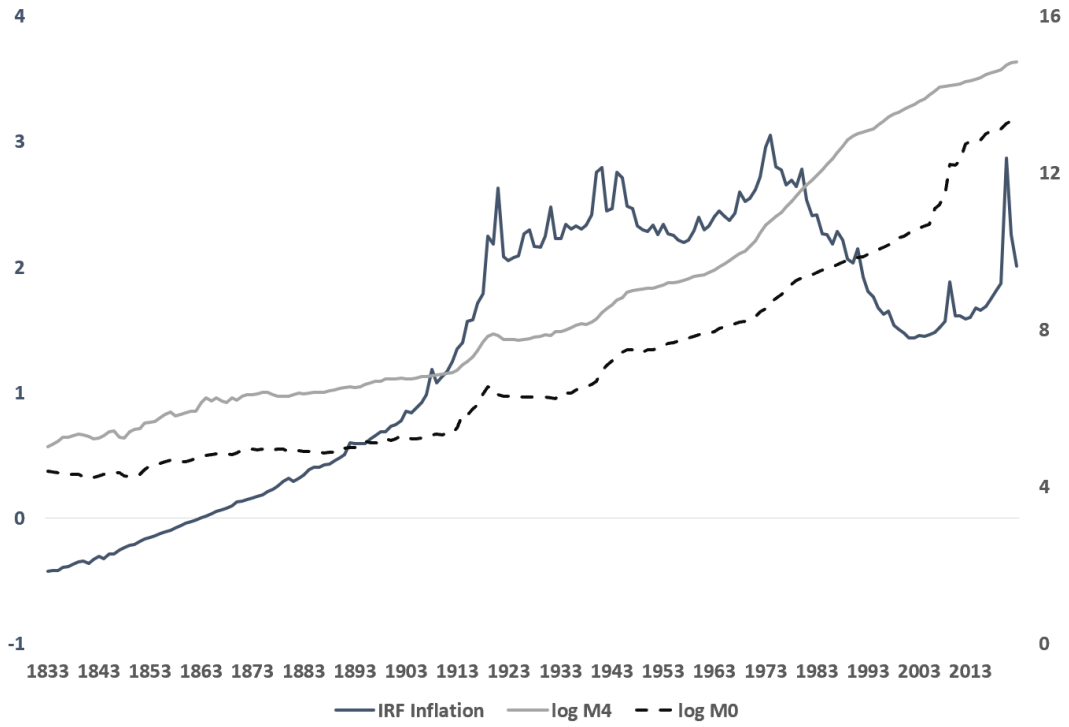

(b) Inflationary effects and credit growth

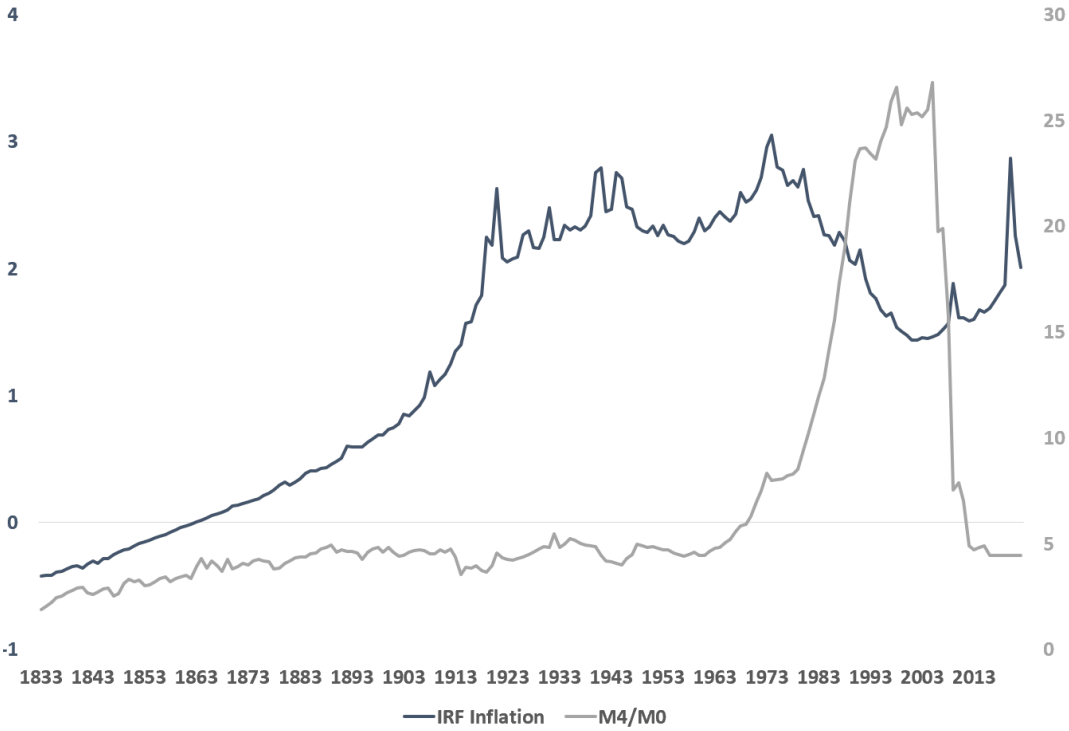

Notes: The blue lines depict the the median IRFs of inflation cumulated over the 5-year horizon and the other lines represent the evolution of two measures of money (M4 and M0) as well as their ratio.

period, the business cycle shock becomes less inflationary, accompanied by a decline in inflation volatility. This observation suggests that the expansion of the financial sector is not the primary driver of inflationary pressure. Instead, the inflationary effects of the business cycle shock in the twentieth century appear to be more closely tied to the growth of base money (M0) rather than to financial development itself.

To summarise, while the significant divergence between M0 and M4 occurred more recently, the M4/M0 ratio rose from 1.9 in 1833 to 4.8 by 1900—a period during which the inflation response shifted from negative to positive. This suggests that the expansion of the money supply, rather than financial development, is the more likely driver of the inflationary nature of business cycle shocks in the twentieth century. Although monetary expansion may result from loose monetary policy, shifts in aggregate demand could also stimulate money growth through changes in money demand. To disentangle these effects, we employ a four-variable VAR model with interest rates and sign restrictions, as discussed in the next section.

Decomposing Aggregate Demand Shocks To separate monetary supply shocks from 'pure' aggregate demand shocks (e.g., shifts in household preferences as described in Smets and Wouters (2007)), we estimate a four-variable VAR that incorporates the nominal interest rate into our baseline empirical model. While the inclusion of interest rates limits the analysis to the post-1700 period, this extension provides valuable insights. Figure 4 presents the forecast error variance decompositions for the four variables in the VAR with sign restrictions.

Despite the wide probability bands, both shocks appear to significantly influence business cycle fluctuations in modern times. The median estimates indicate that pure aggregate demand shocks account for a larger share (20–30%) of output variation compared to money supply shocks (approximately 10–20%). Similarly, pure demand shocks play a more prominent role in explaining price level variation than money supply shocks. In contrast, money supply shocks explain nearly 60% of the variation in money, aligning with the emergence of modern monetary policy. Notably, the real effects of money variation appear

Figure 4: Decomposing aggregate demand: forecast error variance decomposition

(a) Pure aggregate demand shocks

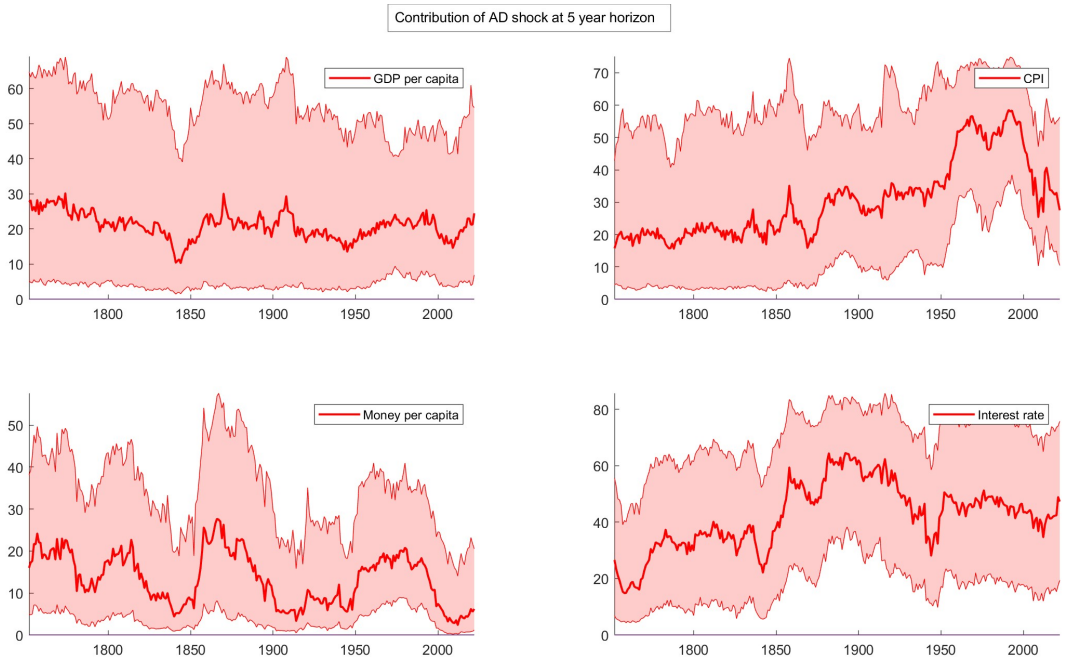

(b) Money supply shocks

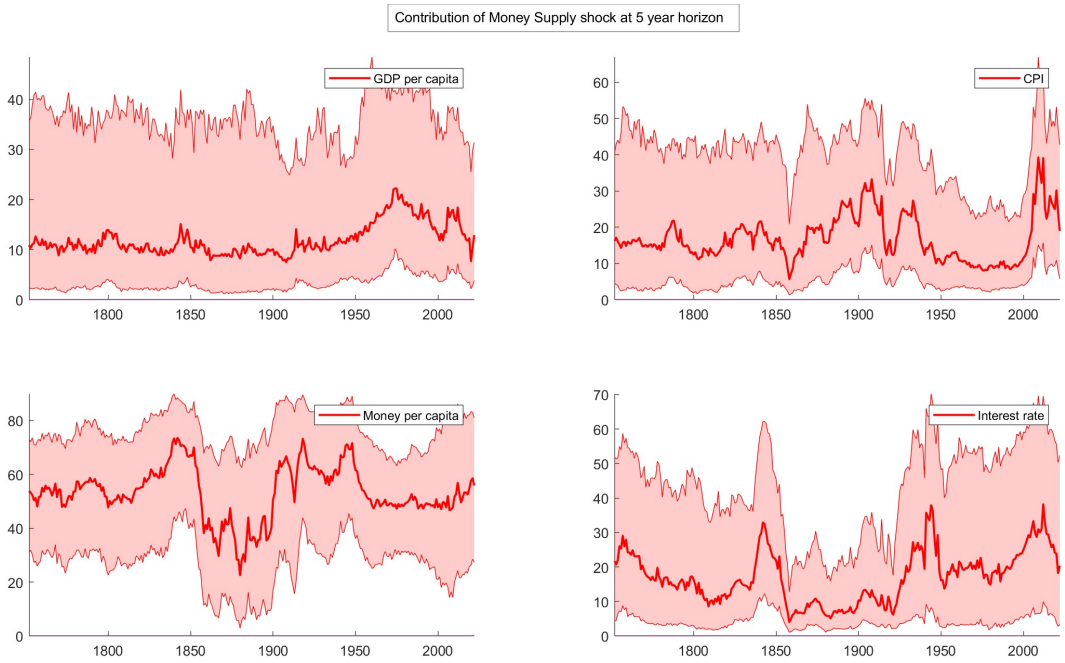

Notes: The pink shaded areas represent the 68 percent credible sets and the red lines depict the medians.

more subdued in modern times compared to the pronounced impacts observed in the 17th century, as discussed earlier.

5 Robustness and extensions

The conclusions reached in the previous section are robust to changes in the information set and even to a change of model. In particular, we replace M0 per capita with a broader measure of money: M4 per capita.[10] Appendix Figure E.4 shows that IRFs under this specification are very similar to the baseline results, with the IRF of M4 shifting slightly upward, especially over the last hundred years. Next, we re-estimate the baseline regression without dividing GDP and M0 by population. Appendix Figure E.8 shows that, once more, IRFs remain very similar to the baseline results.

We also estimate a Dynamic Factor Model (DFM), which allows us to expand the information set and address measurement error in an alternative way. A short description of the model and results is presented in Section E.6. Once more, IRFs are similar to baseline results. Moreover, since our DFM allows an unbalanced panel, we can include Schmelzing (2020)'s measure of long-term real interest rate and estimate the natural rate of interest following Lubik and Matthes (2015). The resulting r-star (shown in Figure E.17) exhibits a declining trend throughout the early centuries of the sample, followed by a long period of relative stability. This stability was disrupted in the late nineteenth century, with the natural rate peaking at 11.5% in 1974.

6 Conclusion

This paper documents how the nature and propagation of business cycle shocks in the UK have evolved over many centuries. We show that pre-modern cycles were dominated by supply-side shocks with stagflationary effects – often linked to climate shocks, demographic events and wars – while modern business cycles are predominantly driven by demand shocks. These findings

[10] Among other holdings, M4 includes private sector's holdings of commercial paper, bonds, Floating Rate Notes and other instruments of up to and including five years' original maturity issued by UK Monetary Financial Institutions.

highlight that business cycle dynamics are not time-invariant but are instead shaped by the prevailing institutional and monetary environment, underscoring the importance of historical perspective in understanding modern macroeconomic fluctuations. Monetisation, for instance, boosted real activity in earlier centuries but became increasingly inflationary as the economy transitioned to a modern monetary system.

We also show that output volatility has declined over time, despite peaking in the seventeenth century, suggesting a centuries-long Great "Moderation", as economic development and stabilising institutions gradually reduced the amplitude of business cycle fluctuations. This historical perspective reveals that even events such as COVID-19 appear less anomalous when viewed against centuries of data. In fact, the volatilities of output and inflation observed during and in the aftermath of COVID-19 are far smaller than the values estimated for the periods before 1700.

Although our analysis is historical, the results carry important policy implications. First, institutional arrangements influence both the types of shocks economies face and the way these shocks propagate. Second, supply-driven stagflationary shocks have historically been the dominant form of macroeconomic disturbance. As shocks related to climate, energy, demographics and immigration become more common, understanding how supply shocks affected the economy in the past can help policymakers better prepare for disturbances whose dynamics may be similar to those of earlier centuries.

References

Abad, L. A. and N. Palma (2021). *The Fruits of the Early Globalization: An Iberian Perspective*, pp. 3–31. Cham: Springer International Publishing. 4

Aghion, P., E. Farhi, and E. Kharroubi (2012, May). Monetary Policy, Liquidity, and Growth. NBER Working Papers 18072, National Bureau of Economic Research, Inc. 8

Aghion, P. and P. Howitt (1992). A model of growth through creative destruction. *Econometrica 60*(2), 323–51. 8

Angeletos, G.-M., F. Collard, and H. Dellas (2020, October). Business-cycle anatomy. *American Economic Review 110*(10), 3030–70. 1, 1, 3.1

Anzoategui, D., D. Comin, M. Gertler, and J. Martinez (2016, February). Endogenous technology adoption and r&d as sources of business cycle persistence. Working Paper 22005, National Bureau of Economic Research. 8

Barsky, R. B. and E. R. Sims (2011). News shocks and business cycles. *Journal of Monetary Economics 58*(3), 273–289. 3.1

Blanchard, O. J. and D. Quah (1989, September). The dynamic effects of aggregate demand and supply disturbances. *American Economic Review 79*(4), 655–73. 1

Bouscasse, P., E. Nakamura, and J. Steinsson (2025). When Did Growth Begin? New Estimates of Productivity Growth in England from 1250 to 1870. *The Quarterly Journal of Economics 140*(2), 835–888. 1

Broadberry, S., B. Campbell, A. Klein, M. Overton, and B. van Leeuwen (2012, January). British Economic Growth, 1270-1870: an output-based approach. Studies in Economics 1203, School of Economics, University of Kent. 4

Broadberry, S., B. M. Campbell, A. Klein, M. Overton, and B. Van Leeuwen (2015). *British Economic Growth, 1270–1870*. Cambridge University Press. 7, E.1

Carter, C. and P. Kohn (2004). On Gibbs sampling for state space models. *Biometrika 81*, 541–53. C.1, C.3

Chahrour, R., S. K. Chugh, and T. Potter (2023, July). Anticipated productivity and the labor market. *Quantitative Economics 14*(3), 897–934. 3.1

Christiano, L. J., R. Motto, and M. Rostagno (2014). Risk shocks. *American Economic Review 104*(1), 27–65. 1, 4

Chu, A. C. and G. Cozzi (2014, May). R&D And Economic Growth In A Cash-In-Advance Economy. *International Economic Review 55*(2), 507–524. 8

Cogley, T., G. E. Primiceri, and T. J. Sargent (2010). Inflation-gap persistence in the us. *American Economic Journal: Macroeconomics 2*(1), 43–69. E.2

Cogley, T. and T. J. Sargent (2005, April). Drift and volatilities: Monetary policies and outcomes in the post wwii u.s. *Review of Economic Dynamics 8*(2), 262–302. 3, B, C.2, E.6

de Vries, J. (2008). *The Industrious Revolution: Consumer Behavior and the Household Economy, 1650 to the Present*. Cambridge: Cambridge University Press. Online publication date: June 2012. 4

Friedman, M. (1956). The quantity theory of money—a restatement. In M. Friedman (Ed.), *Studies in the Quantity Theory of Money*, pp. 3–21. Chicago: University of Chicago Press. 4

Gali, J. (1999, March). Technology, Employment, and the Business Cycle: Do Technology Shocks Explain Aggregate Fluctuations? *American Economic Review 89*(1), 249–271. 1

Geweke, J. (1993). Bayesian treatment of the independent student-t linear model. *Journal of applied econometrics 8*(S1), S19–S40. 3, C.5, C.6

Gil, P. M. and G. Iglesias (2020, August). Endogenous Growth and Real Effects of Monetary Policy: R&D and Physical Capital Complementarities. *Journal of Money, Credit and Banking 52*(5), 1147–1197. 8

Hamilton, E. J. (1934). *American Treasure and the Price Revolution in Spain, 1501-1650*. Classic Reviews in Economic History. Cambridge, MA: Harvard University Press. 4

Hansen, G. D., L. E. Ohanian, and F. Ozturk (2020, November). Dynamic general equilibrium modeling of long and short-run historical events. Working Paper 28090, National Bureau of Economic Research. 1

Jacquier, E., N. Polson, and P. Rossi (1994). Bayesian analysis of stochastic volatility models. *Journal of Business and Economic Statistics 12*, 371–418. C.2

Kim, C.-J. and C. R. Nelson (1999, November). Has The U.S. Economy Become More Stable? A Bayesian Approach Based On A Markov-Switching Model Of The Business Cycle. *The Review of Economics and Statistics 81*(4), 608–616. 1

Koop, G. (2003). *Bayesian Econometrics*. Wiley. B, C.5

Kurmann, A. and C. Otrok (2013, October). News Shocks and the Slope of the Term Structure of Interest Rates. *American Economic Review 103*(6), 2612–32. 3.1

Kurmann, A. and E. Sims (2021, May). Revisions in Utilization-Adjusted TFP and Robust Identification of News Shocks. *The Review of Economics and Statistics 103*(2), 216–235. 3.1

Kydland, F. E. and E. C. Prescott (1982, November). Time to build and aggregate fluctuations. *Econometrica 50*(6), 1345–70. 1

Lubik, T. A. and C. Matthes (2015). Calculating the natural rate of interest: A comparison of two alternative approaches. *Richmond Fed Economic Brief* (Oct). 5, E.6

McCloskey, D. N. (1972). Review of *the price revolution in sixteenth-century england* by Peter H. Ramsey. *Journal of Political Economy 80*(6), 1333–1335. Reprinted from the original publication. 6

McConnell, M. M. and G. Perez-Quiros (2000). Output fluctuations in the United States: what has changed since the early 1980s? *Proceedings* (Mar). 1

Muller, K., C. Xu, M. Lehbib, and Z. Chen (2025, Apr). The global macro database: A new international macroeconomic dataset. NBER Working Papers 33714, National Bureau of Economic Research, Inc. 3

Nason, J. M. and G. W. Smith (2023). UK inflation dynamics since the thirteenth century. *International Economic Review 64*(4), 1595–1614. 1, E.2

Palma, N. (2018a, December). Money and modernization in early modern England. *Financial History Review 25*(3), 231–261. 1, 4

Palma, N. (2018b). Reconstruction of money supply over the long run: the case of England, 1270 - 1870. *Economic History Review 71*(2), 373–392. 1, 4

Palma, N. (2022). The Real Effects of Monetary Expansions: Evidence from a Large-scale Historical Experiment. *The Review of Economic Studies 89*(3), 1593–1627. 1

Parker, G. (2013). *Global Crisis: War, Climate Change and Catastrophe in the Seventeenth Century*. Yale University Press. 1, 4, 5

Perkin, H. J. (1969). *The Origins of Modern English Society, 1780-1880*. London; Toronto: Routledge & Kegan Paul; University of Toronto Press. 4

Primiceri, G. (2005). Time varying structural vector autoregressions and monetary policy. *The Review of Economic Studies 72*(3), 821–52. 1, 3

Ramsey, P. (1971). *The Price Revolution in Sixteenth-Century England*. Debates in Economic History. Methuen Young Books. Hardcover. 4

Reinhart, C. M. and K. S. Rogoff (2008, March). This Time is Different: A Panoramic View of Eight Centuries of Financial Crises. NBER Working Papers 13882, National Bureau of Economic Research, Inc. 1, 4

Reinhart, C. M. and K. S. Rogoff (2013). Shifting Mandates: The Federal Reserve's First Centennial. Technical report. 1, 4

Rogoff, K. S., B. Rossi, and P. Schmelzing (2024, August). Long-Run Trends in Long-Maturity Real Rates, 1311–2022. *American Economic Review 114*(8), 2271–2307. 1

Romer, P. M. (1990, October). Endogenous Technological Change. *Journal of Political Economy 98*(5), 71–102. 8

Schmelzing, P. (2020, January). Eight centuries of global real interest rates, R-G, and the 'suprasecular' decline, 1311–2018. Bank of England working papers 845, Bank of England. 1, 5, E.6, 11

Shapiro, M. D. and M. W. Watson (1988, December). Sources of Business Cycle Fluctuations. In *NBER Macroeconomics Annual 1988, Volume 3*, NBER Chapters, pp. 111–156. National Bureau of Economic Research, Inc. 1

Shi, S. (1997, January). A Divisible Search Model of Fiat Money. *Econometrica 65*(1), 75–102. 9

Smets, F. and R. Wouters (2007, June). Shocks and frictions in us business cycles: A bayesian DSGE approach. *American Economic Review 97*(3), 586–606. 1, 4, 4

Thomas, R. and N. Dimsdale (2018). A millennium of macroeconomic data. Dataset, Bank of England. 2, 11

Uhlig, H. (2004). What moves GNP? In *Econometric Society 2004 North American Winter Meetings*, Number 636. Econometric Society. 3.1

Appendix

A Data

- GDP per capita: the measure of activity is the real GDP (at market prices) per capita. Estimates for 1271-1700 period are only available for England, so we use the estimated real GDP of England throughout the entire sample. For the period where both UK and England GDP series are available – 1700 onwards – the correlation between their growth is very strong: 99%.

- Inflation: the measure of inflation is the CPI variation. For 1271-1869, the series measures the cost of living in England only. For 1870 onwards, it measures inflation in the entire UK.

- Broad Money: the measure of broad money is M4x (M4 excluding intermediate OFCs) from 1997 on; from 1996 to 1963 the variation in M4 is used to backward extrapolate it; from 1962 to 1880, the variation of a synthetic M4 (M3 + building society shares + building society deposits - building societies holdings of cash) is used to construct the series. Then the variation of M3 is applied to construct the series until 1870; and, finally, from 1869 to 1271, the variation of an M3 estimate is used.

- Money: from 1833, the measure of money is the result of the merging of three different series of M0. From 1832 to 1271, the variation of an M3 estimate is used to backward extrapolate this series. Thus, for the first centuries of the sample our measures of money and broad money exhibit the same behaviour.

Figure A.1: Data

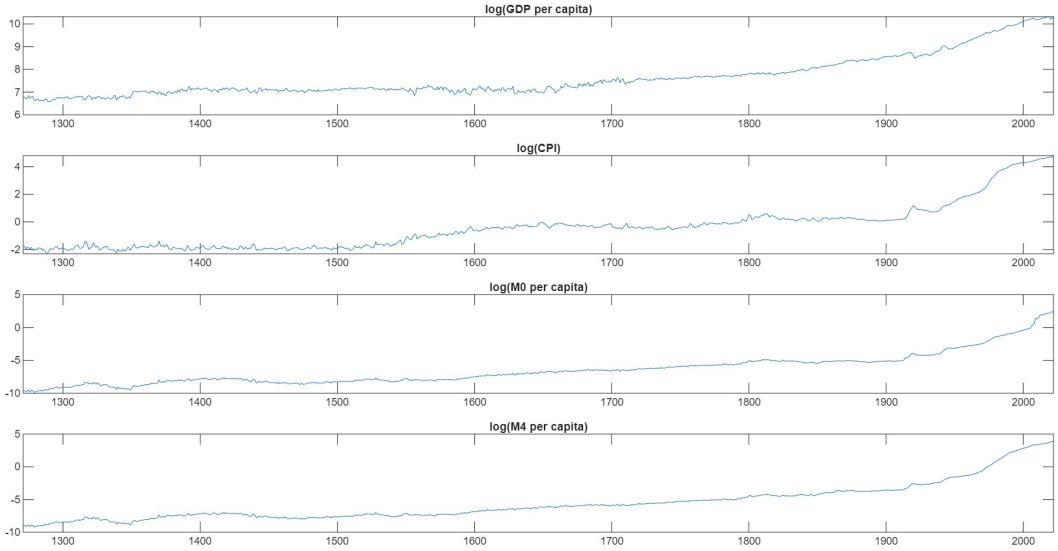

Notes: The blue lines depicts the log of the series used in the estimation.

B Prior distributions and starting values

The initial conditions for the VAR coefficients ϕ_0 are obtained via an OLS estimate of a fixed coefficient VAR using the first 50 observations of the sample period.

Let $\hat{v}^{ols}$ denote the OLS estimate of the VAR covariance matrix estimated on the pre-sample data. For identification, the initial value of the stochastic volatility σ_0^2 is fixed to the diagonal elements of $\hat{v}^{ols}$.

The prior for the off-diagonal elements A_t is $A_0 \sim N\left(\hat{a}^{ols}, V\left(\hat{a}^{ols}\right)\right)$ where $\hat{a}^{ols}$ are the off-diagonal elements of $\hat{v}^{ols}$, with each row scaled by the corresponding element on the diagonal. $V\left(\hat{a}^{ols}\right)$ is assumed to be diagonal with the elements set equal to 10 times the absolute value of the corresponding element of $\hat{a}^{ols}$. The prior on Q is assumed to be inverse Wishart $Q_0 \sim IW\left(\bar{Q}_0, T_0\right)$ where $\bar{Q}_0$ is assumed to be $var(\hat{\phi}^{OLS}) \times 10^{-4}$ and T_0 is the length of the sample used to for calibration. The results are not sensitive to this prior. We obtain similar results for larger values of the scaling parameter. The prior distribution for the blocks of S is inverse Wishart: $S_{i,0} \sim IW(\bar{S}_i, K_i)$ where i indexes the blocks of S. $\bar{S}_i$ is calibrated using $\hat{a}^{ols}$. Specifically, $\bar{S}_i$ is a diagonal matrix with the relevant elements of $\hat{a}^{ols}$ multiplied by 10^{-3}. Following Cogley

and Sargent (2005) we postulate an inverse-gamma distribution for the elements of G, $\sigma_i^2 \sim IG\left(\frac{10^{-4}}{2}, \frac{1}{2}\right)$.

Following Koop (2003), the prior for $\lambda_{k,i} = 1/\varpi_{k,i}$ is gamma

$$p\left(\lambda_k\right) \tilde{\Gamma}\left(1, v_{\lambda,k}\right)$$
$$p\left(v_{\lambda,k}\right) \tilde{\Gamma}\left(v_0, 2\right)$$

where $v_0 = 20$ and $\Gamma\left(a, b\right)$ is the gamma density with mean a and df b.

C Simulating the posterior distribution

We use a Gibbs sampling algorithm to sample from the posterior distribution. The details of each conditional distribution are provided below.

C.1 Time-varying VAR coefficients

Conditional on the time-varying volatilities and contemporaneous coefficients, the model is a SUR system with time-varying parameters. The Carter and Kohn (2004) algorithm is used to sample from the conditional posterior of ϕ_t. The distribution of the time-varying VAR coefficients ϕ_t conditional on all other parameters and hyperparameters is linear and Gaussian: $\phi_t \backslash Z_t, \Xi \sim N\left(\phi_{T\backslash T}, P_{T\backslash T}\right)$ and $\phi_t \backslash \phi_{t+1}, Z_t, \Xi \sim N\left(\phi_{t\backslash t+1,\phi_{t+1}}, P_{t\backslash t+1,\phi_{t+1}}\right)$ where $t = T-1, ..1$, Ξ denotes a vector that holds all the other VAR parameters and $\phi_{T\backslash T} = E\left(\phi_T \backslash Z_t, \Xi\right), P_{T\backslash T} = Cov\left(\phi_T \backslash Z_t, \Xi\right), \phi_{t\backslash t+1,\phi_{t+1}} = E\left(\phi_t \backslash Z_t, \Xi, \phi_{t+1}\right)$ and $P_{t\backslash t+1,F_{t+1}} = Cov\left(\phi_t \backslash Z_t, \Xi, \phi_{t+1}\right)$. As shown by Carter and Kohn (2004) the simulation proceeds as follows. First we use the Kalman filter to draw $\phi_{T\backslash T}$ and $P_{T\backslash T}$ and then proceed backwards in time using $\phi_{t|t+1} = \phi_{t|t} + P_{t|t}P_{t+1|t}^{-1}\left(\phi_{t+1} - \phi_t\right)$ and $\phi_{t|t+1} = \phi_{t|t} - P_{t|t}P_{t+1|t}^{-1}P_{t|t}$.

C.2 Elements of H_t

Following Cogley and Sargent (2005), the diagonal elements of the VAR covariance matrix are sampled using the Metropolis Hastings algorithm in Jacquier et al. (1994). Given a draw for ϕ_t

the VAR model can be written as $A_t'\left(\tilde{Z}_t\right) = u_t$. where $\tilde{Z}_t = Z_t - \sum_{l=1}^{L} \phi_{l,t} Z_{t-l} = v_t$ and $VAR(u_t) = H_t$. Jacquier et al. (1994) note that conditional on other VAR parameters, the distribution $h_{it}, i = 1..N$ is given by $f(h_{it} \backslash h_{it-1}, h_{it+1}, u_{it}) = f(u_{it} \backslash h_{it}) \times f(h_{it} \backslash h_{it-1}) \times f(h_{it+1} \backslash h_{it}) = h_{it}^{-0.5} \exp\left(\frac{-u_{it}^2}{2h_{it}}\right) \times h_{it}^{-1} \exp\left(\frac{-(\ln h_{it} - \mu)^2}{2\sigma_{h_i}}\right)$ where μ and σ_{h_i} denote the mean and the variance of the log-normal density $h_{it}^{-1} \exp\left(\frac{-(\ln h_{it} - \mu)^2}{2\sigma_{h_i}}\right)$. Jacquier et al. (1994) suggest using $h_{it}^{-1} \exp\left(\frac{-(\ln h_{it} - \mu)^2}{2\sigma_{h_i}}\right)$ as the candidate generating density with the acceptance probability defined as the ratio of the conditional likelihood $h_{it}^{-0.5} \exp\left(\frac{-u_{it}^2}{2h_{it}}\right)$ at the old and the new draw. This algorithm is applied at each period in the sample.

C.3 Elements of A_t

Given a draw for ϕ_t the VAR model can be written as $A_t'\left(\tilde{Z}_t\right) = u_t$ where $\tilde{Z}_t = Z_t - \sum_{l=1}^{L} \phi_{l,t} Z_{t-l} = v_t$ and $VAR(u_t) = H_t$. This is a system of equations with time-varying coefficients and given a block diagonal form for $Var(\tau_t)$ the standard methods for state space models described in Carter and Kohn (2004) can be applied.

C.4 VAR hyperparameters

Conditional on Z_t, $\phi_{l,t}$, H_t, and A_t, the innovations to $\phi_{l,t}$, H_t, and A_t are observable, which allows us to draw the hyperparameters—, the elements of Q, S, and the σ_i^2—, from their respective distributions.

C.5 Elements of λ_t

The conditional posterior distributions related to the t-distributed shock structure of the model are described in Koop (2003). Note that conditional on Φ_t and A_t, the orthogonalized residuals can be obtained as $\tilde{\varepsilon}_t = A_t u_t$. The conditional posterior distribution for $\lambda_{i,t}$ derived in Geweke (1993) applies to each column of $\tilde{\varepsilon}_t$. As shown in Koop (2003)this posterior density is a gamma distribution with mean $(v_{\lambda,i} + 1) / \frac{1}{\sigma_{i,t}} \tilde{\varepsilon}_{i,t}^2 + v_{\lambda,i}$ and degrees of freedom $v_{\lambda,i} + 1$. Note that $\tilde{\varepsilon}_{i,t}$ is the ith column of the matrix $\tilde{\varepsilon}_t$.

C.6 Degrees of freedom $v_{\lambda,i}$

The conditional distribution for the degree of freedom parameter is non-standard and given by:

$$G\left(v_{\lambda,i}\backslash\lambda_i\right) \propto \left(\frac{v_{\lambda,i}}{2}\right)^{\frac{Tv_{\lambda,n}}{2}} \Gamma\left(\frac{v_{\lambda,n}}{2}\right)^{-N} \exp\left(-\left(\frac{1}{v_0}+0.5\sum_{t=1}^{T}\left[\ln\left(\lambda_{t,n}^{-1}\right)+\lambda_{t,n}\right]\right)v_{\lambda,n}\right) \tag{C.1}$$

As in Geweke (1993) we use the Random Walking Metropolis Hastings Algorithm to draw from this conditional distribution. More specifically, for each of the n equations of the VAR, we draw $v_{\lambda,n}^{new} = v_{\lambda,n}^{old} + c^{1/2}\epsilon$ with $\epsilon \sim N(0,1)$. The draw is accepted with probability $\frac{G\left(v_{\lambda,n}^{new}\backslash\lambda_n\right)}{G\left(v_{\lambda,n}^{old}\backslash\lambda_n\right)}$ with c chosen to keep the acceptance rate between 20% and 40%.

D The Gibbs sampling algorithm

The Gibbs algorithm for the model cycles through the following eight conditional posterior distributions:

1. $G(\lambda_{i,t}\backslash\Psi)$ where Ψ denotes the remaining parameters of the model.
2. $G\left(v_{\lambda,i}\backslash\lambda_{i,t}\right)$
3. $G\left(g_{i,t}\backslash\Psi\right)$
4. $G\left(\sigma_{i,t}^2\backslash\Psi\right)$
5. $G\left(A_t\backslash\Psi\right)$
6. $G\left(\Phi_t\backslash\Psi\right)$
7. $G\left(Q\backslash\Psi\right)$
8. $G\left(Q_A\backslash\Psi\right)$

E Additional results

E.1 Matching the Business Cycle Shocks with Narrative Accounts

This figure shows that during episodes such as the Elizabethan famine (1594–1597), the English Civil War (1642–1651), the Napoleonic Wars (1812–1814), the 1816 crop failure, and the Irish Famine (1845–1852), the model consistently identifies large negative business cycle shocks. These are characterized by declining output and rising prices, confirming the supply-side nature of macroeconomic disruptions in this era (Broadberry et al. (2015)).

Figure E.1: Narrative evidence

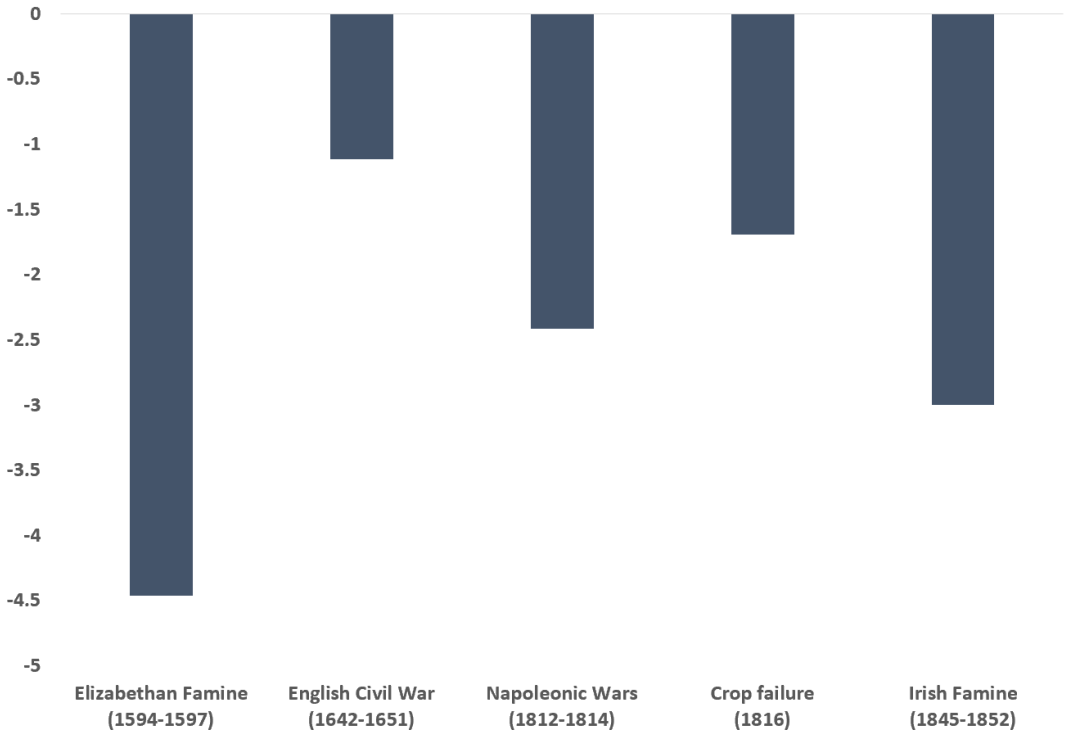

Notes: The bars show the main business cycle shocks cumulated over the years for several famous episodes of British history.

E.2 Predictability

We also examine the predictability of output, inflation, and money using forecast R^2 (Cogley et al., 2010) from the VAR model. As shown in Figure E.2, the rise in inflation predictability is a relatively recent phenomenon, consistent with the findings of Cogley et al. (2010) for post-war U.S. data. Similar to Nason and Smith (2023), we find that inflation predictability

remained low throughout earlier centuries. Predictability increases substantially in the twentieth century. Output, on the other hand, shows a contrasting trend: output predictability has actually declined since the 1300s with the exception of the Great Financial Crisis.

Figure E.2: Predictability

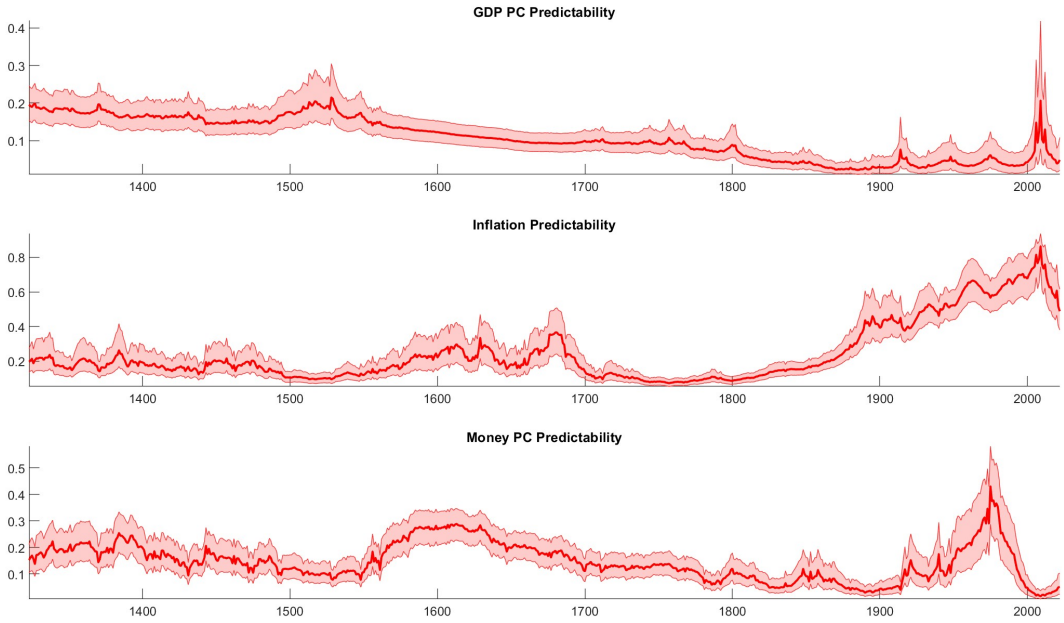

Notes: The pink shaded areas represent the 68 percent credible sets and the red lines depict the medians.

E.3 Three-variable VAR with M4

Figure E.3: Stochastic Volatility

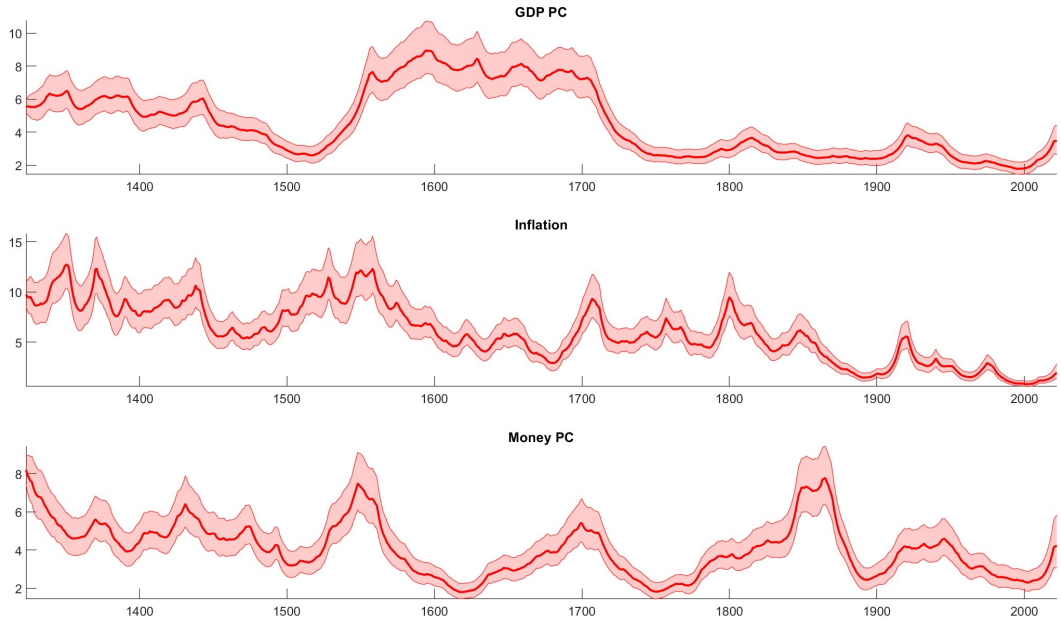

Notes: The pink shaded areas represent the 68 percent credible sets and the red lines depict the medians.

Figure E.4: Impulse responses

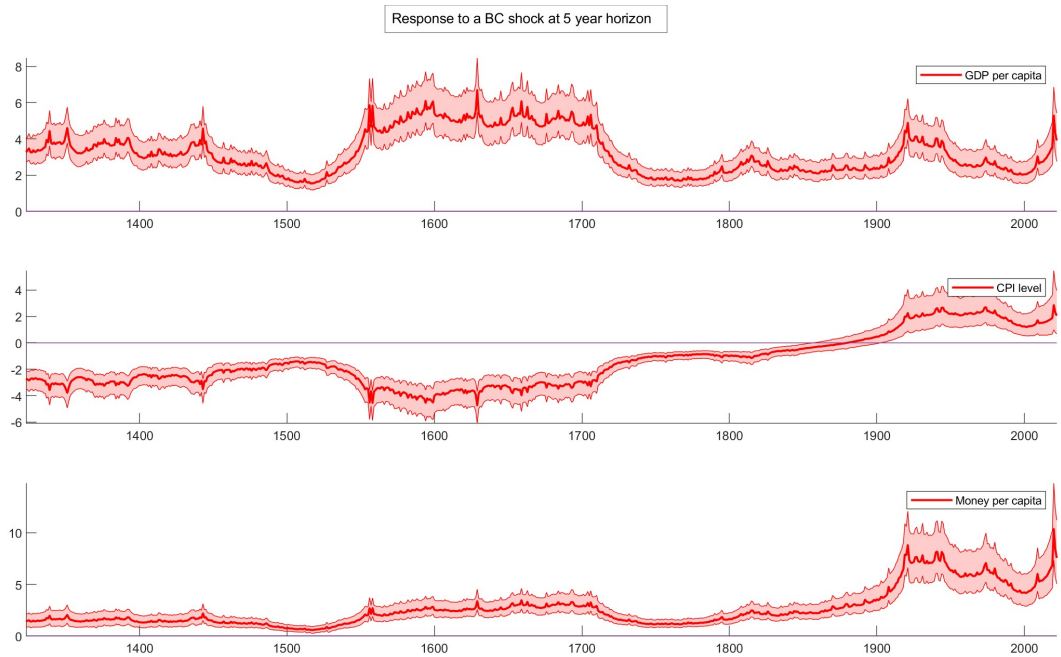

Notes: The pink shaded areas represent the 68 percent credible sets for the IRFs and the red lines depict the median IRFs using M4 as the measure of money.

Figure E.5: Conditional Volatility

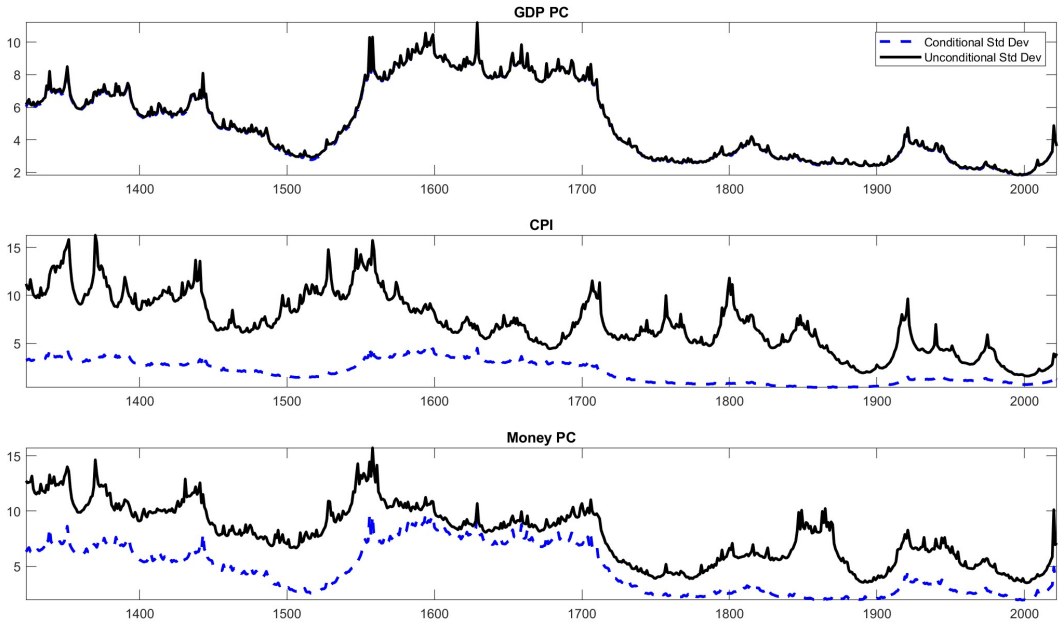

Notes: The dashed blue lines are the estimates of the time-varying volatilities of each variable conditional on the business cycle shock. The solid black lines are the estimates of the unconditional volatilities of each of these variables.

Figure E.6: Predictability

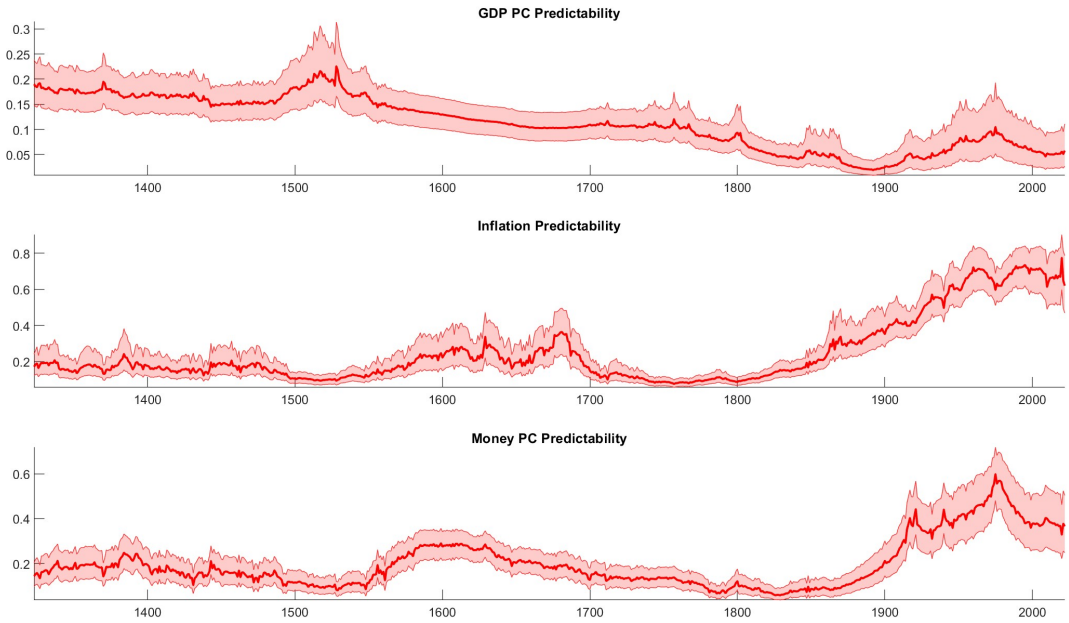

Notes: The pink shaded areas represent the 68 percent credible sets and the red lines depict the medians.

E.4 Three-variable VAR using aggregate (non-per-capita) variables

Figure E.7: Stochastic Volatility

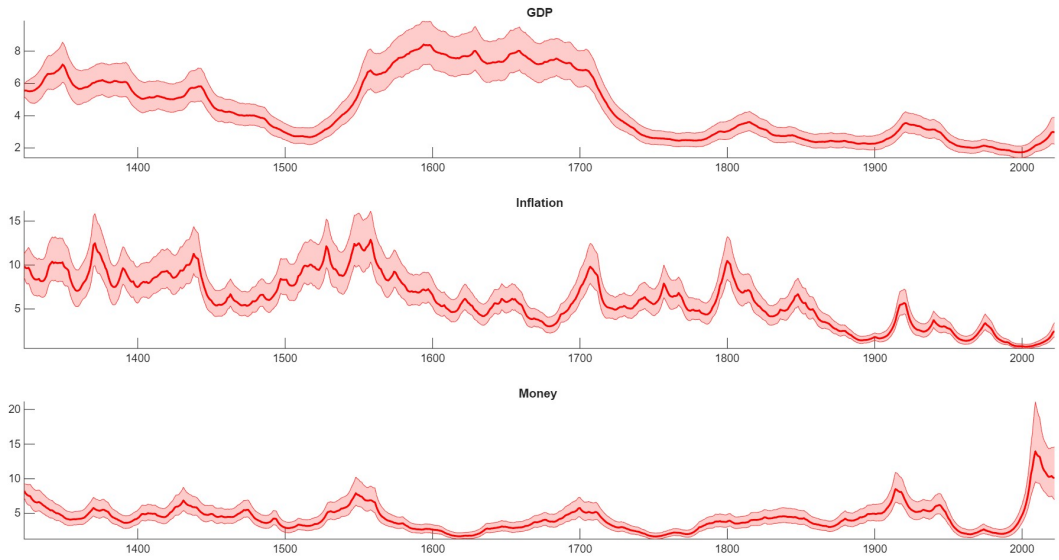

Notes: The pink shaded areas represent the 68 percent credible sets and the red lines depict the medians.

Figure E.8: Impulse responses

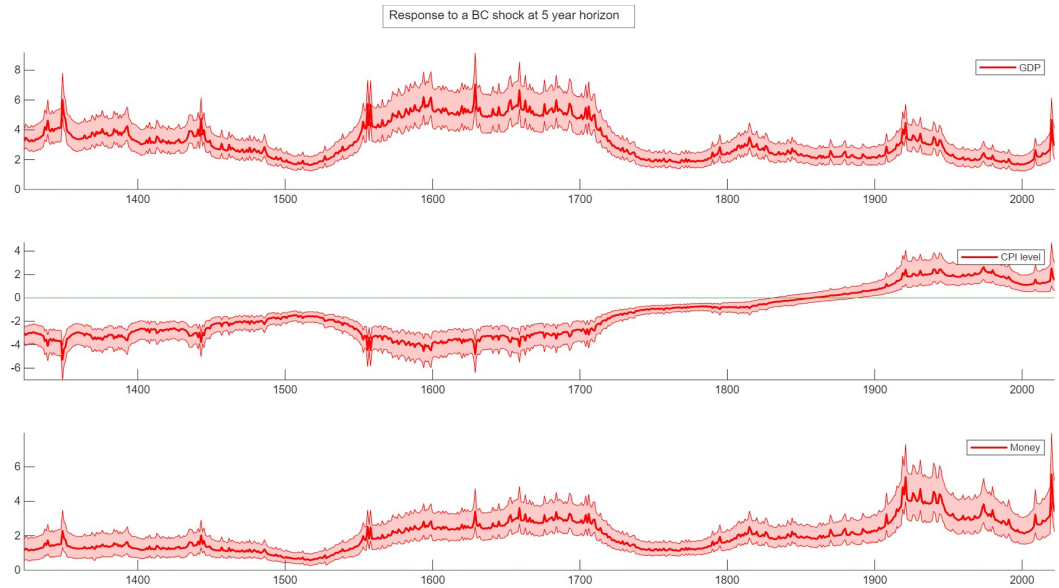

Notes: The pink shaded areas represent the 68 percent credible sets for the IRFs and the red lines depict the median IRFs using aggregate (non-per-capita) variables.

Figure E.9: Predictability

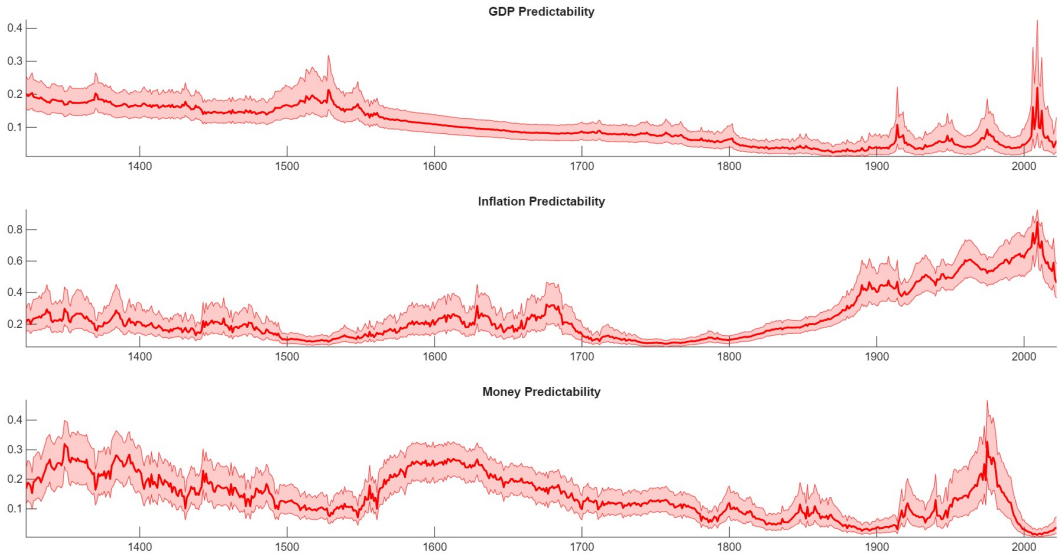

Notes: The pink shaded areas represent the 68 percent credible sets and the red lines depict the medians.

E.5 Extra sign restriction plots

Figure E.10: IRF: aggregate demand

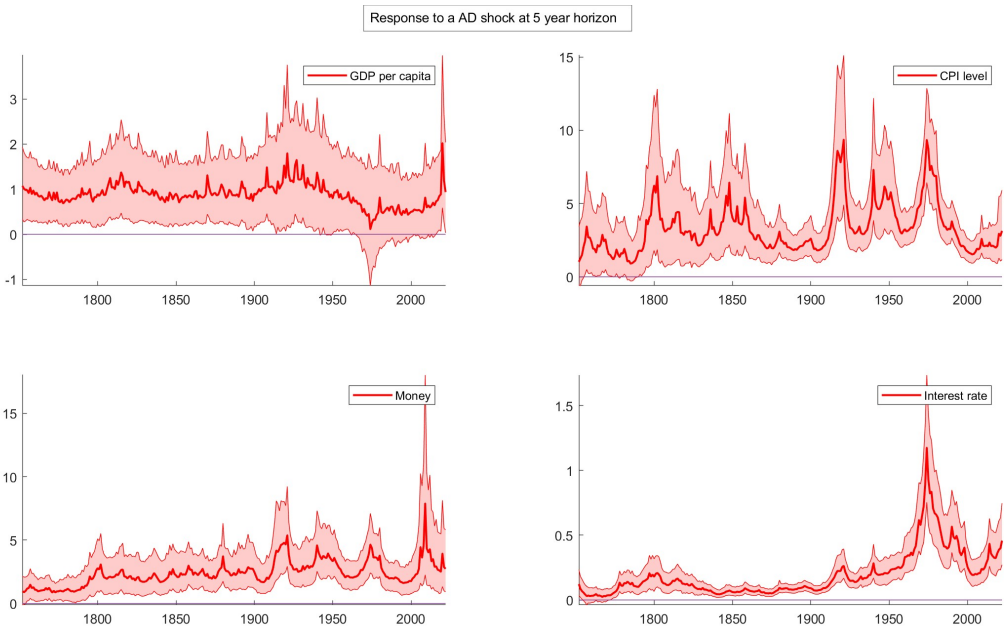

Notes: The pink shaded areas represent the 68 percent credible sets for the IRFs and the red lines depict the median IRFs using sign restrictions.

Figure E.11: IRF: aggregate supply

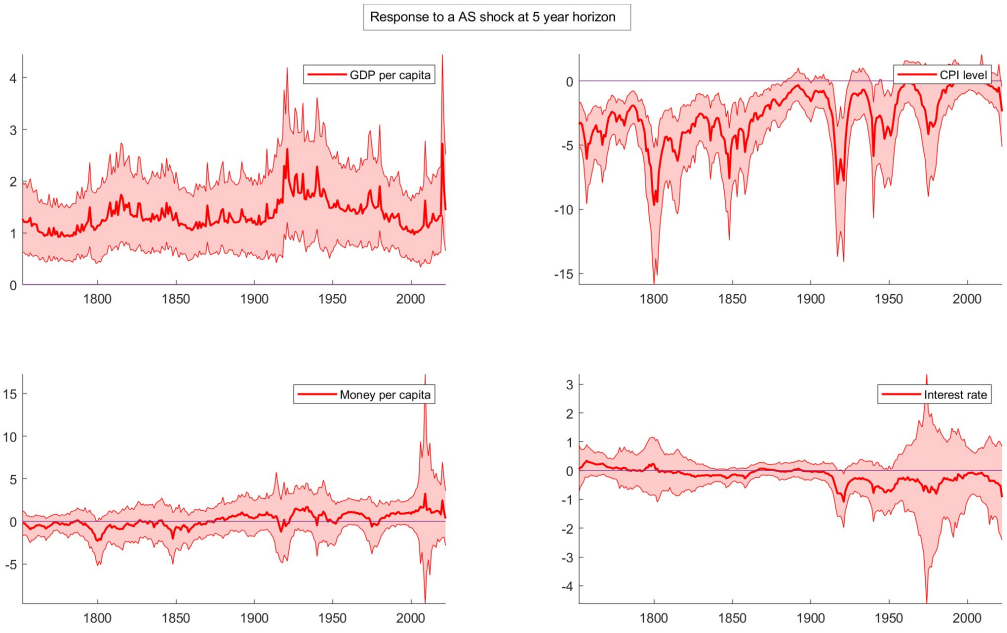

Notes: The pink shaded areas represent the 68 percent credible sets for the IRFs and the red lines depict the median IRFs using sign restrictions.

Figure E.12: IRF: money demand

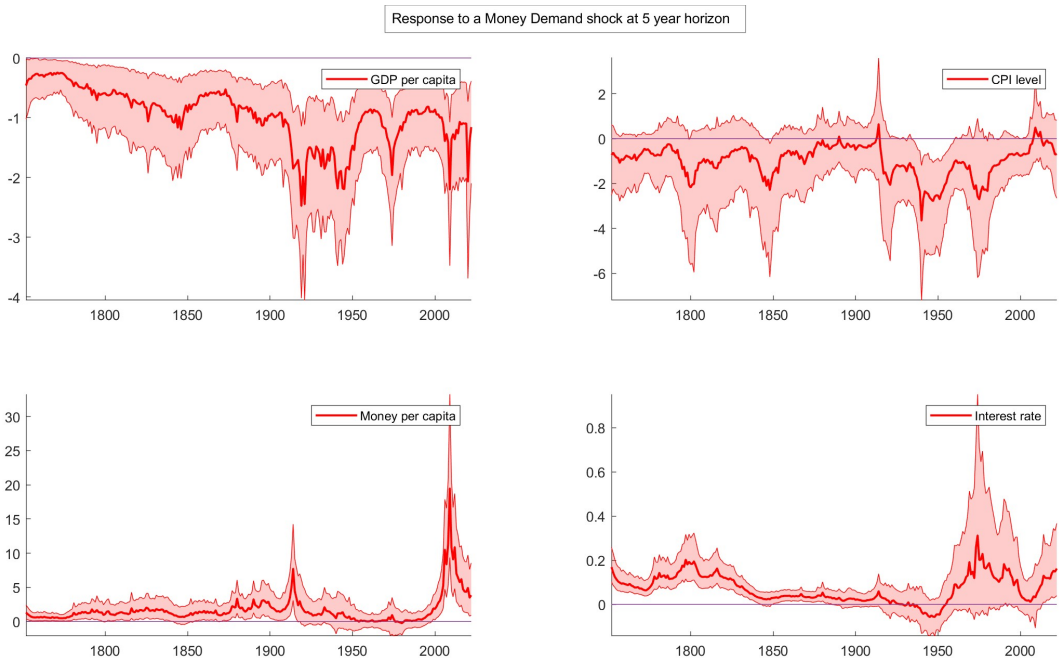

Notes: The pink shaded areas represent the 68 percent credible sets for the IRFs and the red lines depict the median IRFs using sign restrictions.

Figure E.13: IRF: money supply

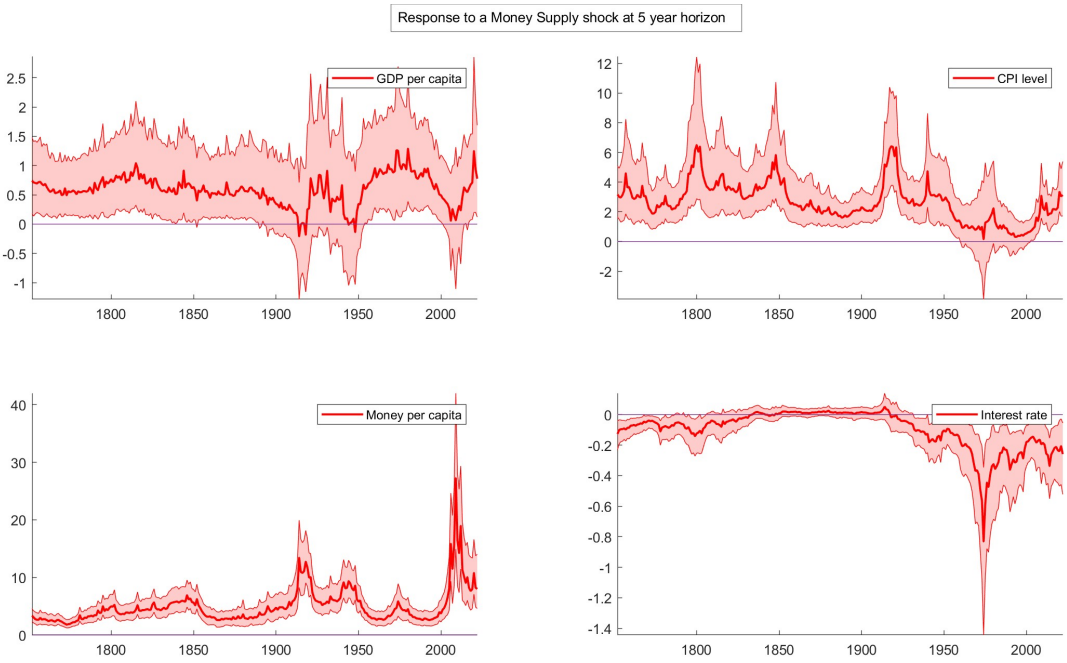

Notes: The pink shaded areas represent the 68 percent credible sets for the IRFs and the red lines depict the median IRFs using sign restrictions.

Figure E.14: FEVD: aggregate supply

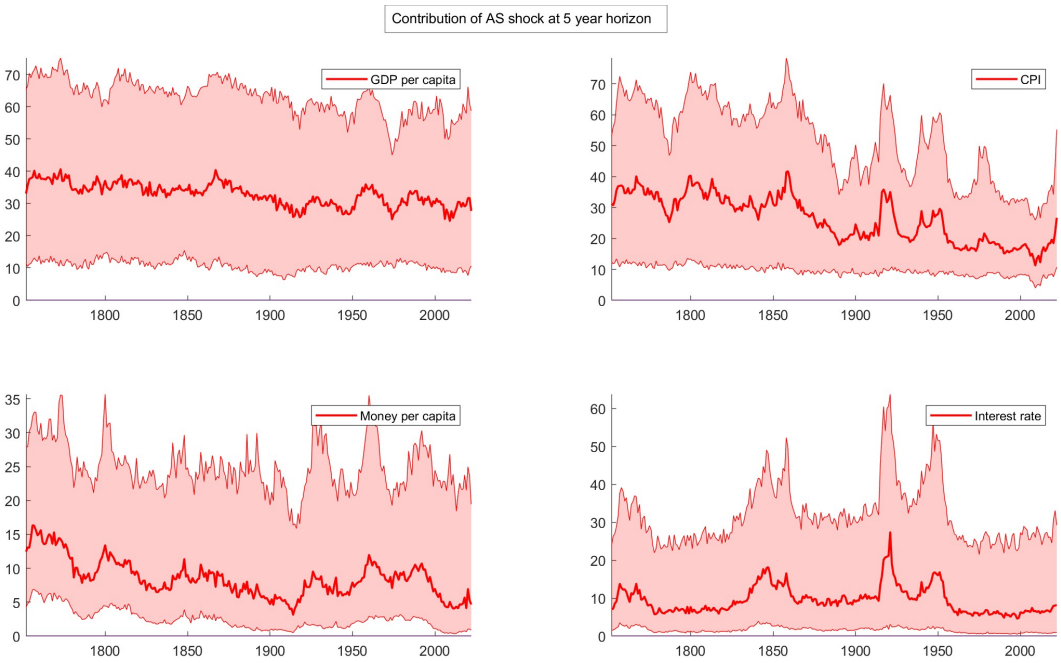

Notes: The pink shaded areas represent the 68 percent credible sets and the red lines depict the medians.

Figure E.15: FEVD: money demand

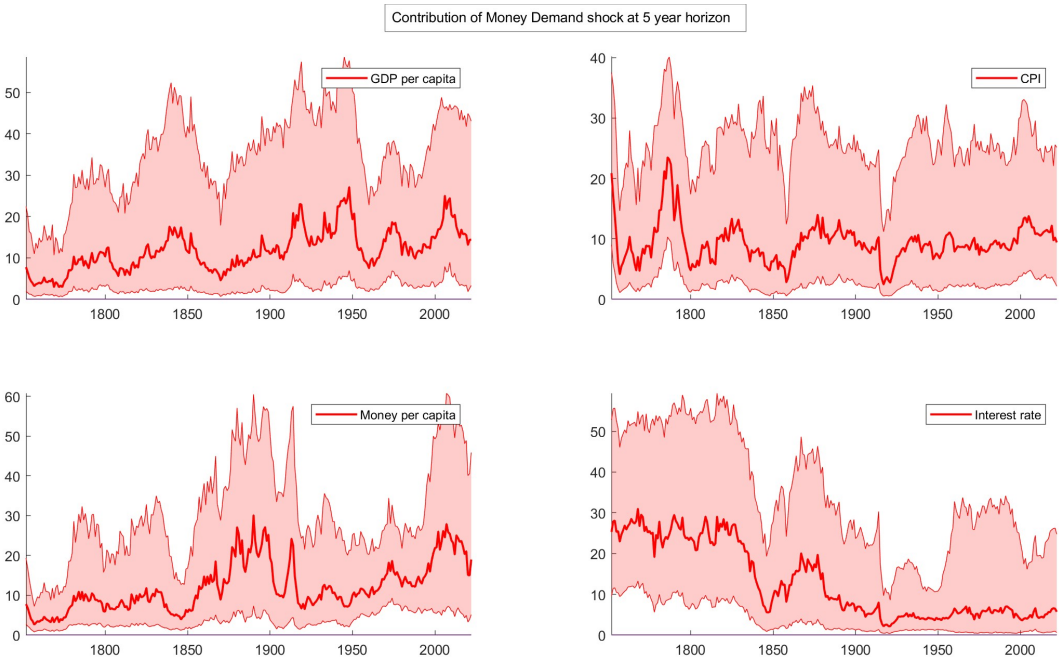

Notes: The pink shaded areas represent the 68 percent credible sets and the red lines depict the medians.

E.6 Dynamic Factor Model

Alternatively, we address measurement error by estimating a Dynamic Factor Model (DFM). Figure E.16 shows that IRFs are similar to baseline results. A by-product of this approach is an estimate of the natural rate of interest. Following Lubik and Matthes (2015), we estimate r-star as the 5-year-ahead forecast of the observed real interest rate. Figure E.17 shows this estimate for the UK over seven centuries. In line with Schmelzing (2020), our estimate exhibits a declining trend throughout the early centuries of the sample, followed by a long period of relative stability. This stability was disrupted in the late nineteenth century, with the natural rate peaking at 11.5% in 1974.

Figure E.16: Main IRFs from DFM model

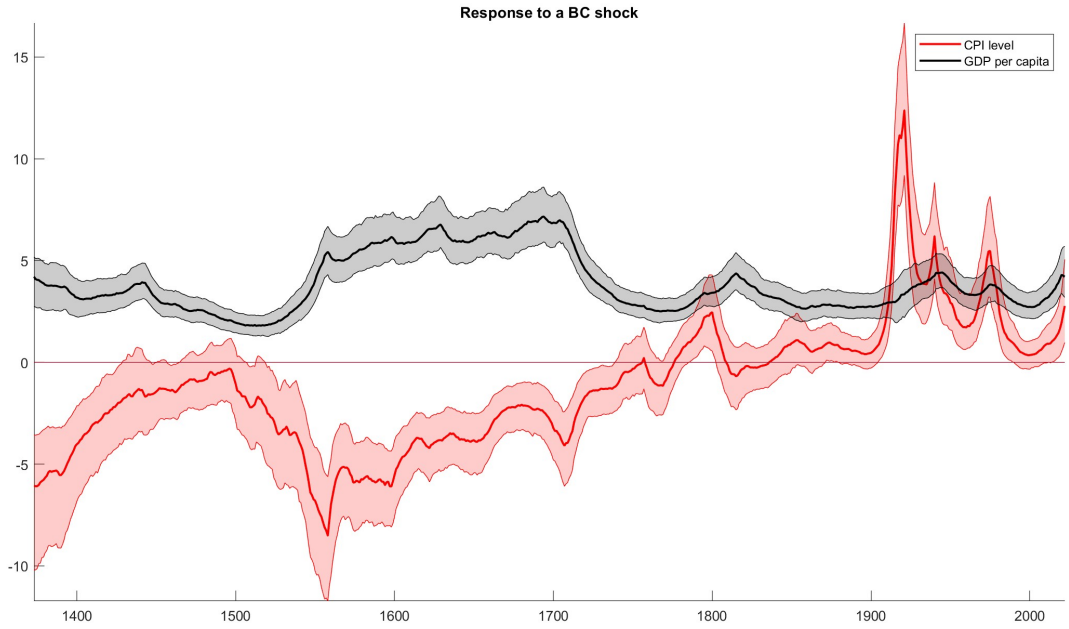

Notes: The pink shaded area represents the 68 percent credible set and the red line depicts the median IRFs of CPI produced by a DFM. The grey shaded area and the black line display the equivalent quantities for the GDP per capita.

Figure E.17: Estimated Natural Rate

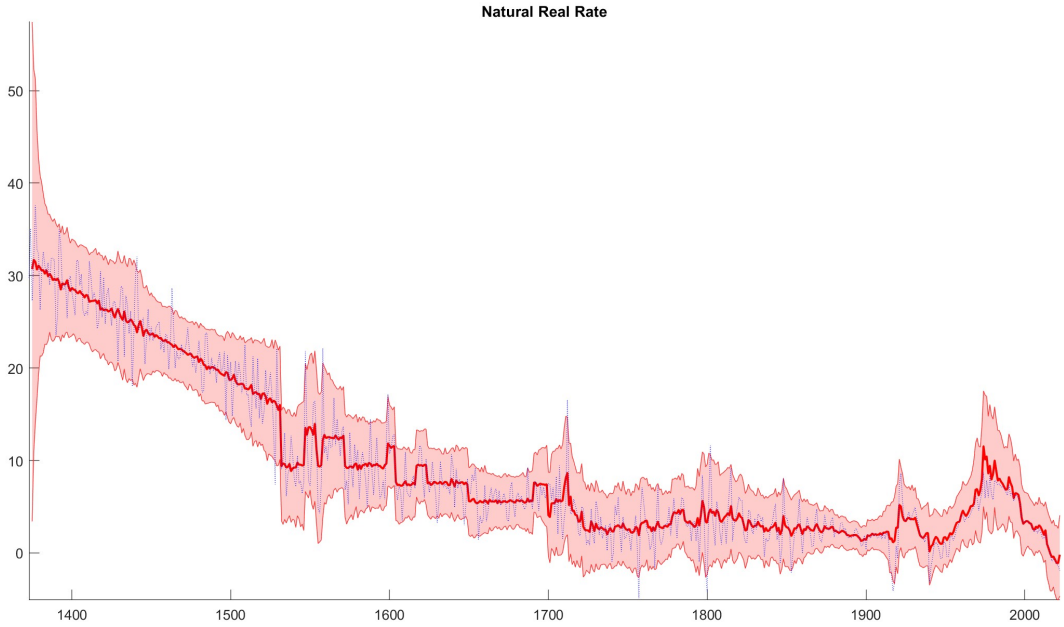

Notes: The pink shaded area represents the 68 percent credible set and the red line is the median natural rate of interest.

Estimation and specification We model the dynamics of 11 variables denoted by $\underset{M\times 1}{X_t}$ using a Dynamic Factor model with time-varying parameters that allows for an unbalanced panel. These variables are: real wages, GDP deflator, CPI, exports, commodity prices, GDP, GDP per capita, M4, shares prices, the dollar rate and the real interest rate.[11] Variables are included in the model in first differences, with the exception of the interest rate.

The observation equation of the model is defined as:

$$X_t = BF_t + v_t$$

$$v_t = \rho v_{t-1} + \sigma_t^{\frac{1}{2}} e_t$$

$$ln(\sigma_t) = ln(\sigma_{t-1}) + g_t$$

F_t denotes k common factors in the dataset X_t, and the idiosyncratic components e_t accounts for measurement error.

[11]The real interest rate is obtained from Schmelzing (2020) and the other variables are obtained from Thomas and Dimsdale (2018) as before.

The transition equation is:

$$F_t = \beta_t F_{t-1} + A_t^{-1} H_t^{\frac{1}{2}} \epsilon_t$$

$$\tilde{\beta}_t = \tilde{\beta}_{t-1} + u_{\beta,t}$$

$$h_t = h_{t-1} + u_{h,t}$$

$$a_t = a_{t-1} + u_{a,t}$$

The model is estimated using an MCMC algorithm. Priors for $var(u_{\beta,t})$, $var(u_{h,t})$ and $var(g_t)$ are based on previous studies such as Cogley and Sargent (2005) like in the VAR.

School of Economics and Finance

Queen Mary
University of London

School of Economics and Finance
Queen Mary University of London
Mile End Road
London E1 4NS
Tel: +44 (0)20 7882 7356
Fax: +44 (0)20 8983 3580
Web: www.econ.qmul.ac.uk/research/workingpapers/